University of California

Ernest O. Lawrence Radiation Laboratory

THE REACTION $K^-p \rightarrow \Lambda\eta$ FROM 1.2 TO 1.7 BeV/c

Berkeley, California

Submitted to Physical Review

UCRL-17515
Preprint

UNIVERSITY OF CALIFORNIA

Lawrence Radiation Laboratory
Berkeley, California

AEC Contract No. W-7405-eng-48

THE REACTION $K^-p \rightarrow \Lambda\eta$ FROM 1.2 TO 1.7 BeV/c

Stanley M. Flatté and Charles G. Wohl

April 24, 1967

The Reaction $K^-p \rightarrow \Lambda\eta$ from 1.2 to 1.7 BeV/c*

Stanley M. Flatté and Charles G. Wohl

Lawrence Radiation Laboratory
University of California
Berkeley, California

April 24, 1967

ABSTRACT

Total and differential cross sections of the reaction $K^-p \rightarrow \Lambda\eta$ have been determined for incident K^- lab momenta between 1.2 and 1.7 BeV/c. No striking resonance formation in the direct channel is seen; in particular, the $Y_0^*(2100)$ decays not more than 3% via the $\Lambda\eta$ channel. A prominent forward peak in the differential cross sections indicates some crossed-channel meson-exchange activity. The branching ratio $\Gamma(\eta \rightarrow \text{neutrals})/\Gamma(\eta \rightarrow \pi^+\pi^-\pi^0)$ is 3.6 ± 0.6.

I. INTRODUCTION

We have analyzed more than 1000 $K^-p \to \Lambda\eta$ events at five momenta between 1.2 and 1.7 BeV/c. The reaction was observed in two different modes in the 72-in. hydrogen bubble chamber:

(a) $K^-p \to \Lambda\eta \to (p\pi^-)(\pi^+\pi^-\pi^0)$, which resulted in V + two-prong events, and

(b) $K^-p \to \Lambda\eta \to (p\pi^-)$(neutrals), which resulted in V + zero-prong events.

Section II describes the analysis of the V + two-prongs; Sec. III describes the analysis of the V + zero-prongs, and Sec. IV gives the combined results.

Our conclusions, set forth in Sec. V, may be summarized as follows:

1. No striking resonance phenomena are evident in the $\Lambda\eta$ system near these momenta; in particular, the $Y_0^*(2100)$ decays not more than 3% via the $\Lambda\eta$ channel.

2. The differential cross sections exhibit a prominent forward peak, indicating the presence of meson exchanges.

3. The branching ratio $\Gamma(\eta \to \text{neutrals})/\Gamma(\eta \to \pi^+\pi^-\pi^0)$ is 3.6 ± 0.6.

II. ANALYSIS OF V + TWO-PRONG EVENTS ($K^-p \to \Lambda\pi^+\pi^-\pi^0$)

The method for identifying events of the type $K^-p \to \Lambda\pi^+\pi^-\pi^0 \to (p\pi^-)(\pi^+\pi^-\pi^0)$ in our experiment has been given in a previous publication.[1] We have approximately 9000 events of this type. The three-pion mass spectra show a prominent η peak at each momentum (Fig. 1). In order to estimate the number of η's we assumed a linear background over the mass region 505 to 595 MeV, and used the formula

$$N_\eta = N_{3\pi}(535 \text{ to } 565 \text{ MeV}) - 1/2[N_{3\pi}(505 \text{ to } 535 \text{ MeV}) + N_{3\pi}(565 \text{ to } 595 \text{ MeV})],$$

with appropriate error treatment.

The only analysis question that remains involves the $\pi^+\pi^-\gamma$ decay mode of the η. How much of this decay mode has contaminated our sample of $\eta \to \pi^+\pi^-\pi^0$ events? To find an answer we plotted the mass squared of the system recoiling against the $\Lambda\pi^+\pi^-$ system for our η events. Background was subtracted for each bin in the manner described in an earlier publication.[2] The resulting graph, Fig. 2, shows no sign of a peak at the γ-ray mass squared, and fits the experimental resolution function with the center at the π^0 mass squared. However, because of poor statistics we cannot set a very small upper limit on the $\pi^+\pi^-\gamma$ contamination from this figure.

To do better we used the program FAKE[3] to generate $K^-p \to \Lambda(\eta \to \pi^+\pi^-\gamma$ and $\pi^+\pi^-\pi^0)$ events with the same production-angle distribution as that of the η's in our experiment. When our normal selection criteria were applied to these fake events, 99% of the $\Lambda\pi^+\pi^-\pi^0$ events passed, while only 0.8% of the $\Lambda\pi^+\pi^-\gamma$ events passed. Since the $\pi^+\pi^-\gamma$ mode of the η has a rate of about one-fifth that of the

$\pi^+\pi^-\pi^0$ mode, we conclude that less than 0.2% of our $\eta \to \pi^+\pi^-\pi^0$ sample consists of misidentified $\eta \to \pi^+\pi^-\gamma$ events.

In Table I we give our estimates of the number of η's at each momentum, and the cross section for $K^-p \to \Lambda\eta$, where we have used the branching ratio[4] $\Gamma(\eta \to \pi^+\pi^-\pi^0)/\Gamma(\eta \to \text{all}) = 0.224$.

We also determined an average cross section over our sample for the reaction $K^-p \to \Lambda\eta \to (p\pi^-)(\pi^+\pi^-\pi^0)$ of 37 ± 3 μb. In Sec. IV we combine this result with a similar cross section for $K^-p \to \Lambda\eta \to (p\pi^-)(\text{neutrals})$ to obtain the branching ratio $\Gamma(\eta \to \text{neutrals})/\Gamma(\eta \to \pi^+\pi^-\pi^0)$.

We have determined the production-angle distributions for $K^-p \to \Lambda\eta \to \Lambda\pi^+\pi^-\pi^0$ in the same manner as described in Ref. 2 for $K^-p \to \Lambda\omega$ events. Background was subtracted in each angular bin; however, we assumed that the background for the η's is linear from 505 to 595 MeV, rather than drawing a background curve by eye as was done in the ω case. Our results, combined with those of Sec. III, are presented in Sec. IV.

We have too few events to determine the polarization state of the Λ at all momenta and production angles. However, we can give two statistically significant results, both at 1.51 BeV/c. Let P_Λ be the polarization of the Λ along the normal to the plane of production (the only polarization allowed by parity conservation). Then, in the Λ rest frame, the distribution of the momentum of the pion from the Λ decay is given by the expression $[1 - \alpha_\Lambda P_\Lambda \pi_\Lambda \cdot (K^- \times \eta)/|K^- \times \eta|]$. This expression provides a simple experimental convention for $\alpha_\Lambda P_\Lambda$. Our results, for $K^-p \to \Lambda\eta \to \Lambda\pi^+\pi^-\pi^0$ events at 1.51 BeV/c, are $\alpha_\Lambda P_\Lambda = -0.2 \pm 0.3$ for

$\cos\theta_{K\eta} > 0.8$ (events in the forward peak), and $\alpha_\Lambda P_\Lambda = +0.4 \pm 0.2$ for $\cos\theta_{K\eta} < 0.8$.

III. ANALYSIS OF V + ZERO-PRONG EVENTS ($K^-p \rightarrow \Lambda$ + neutrals)

Figure 3 shows the distribution of events in which the V is a $\Lambda \rightarrow p\pi^-$ decay, plotted against the square of the invariant mass of the system of undetected neutral particles recoiling against the Λ. Only events with a Λ length greater than 5 mm before decay and with production and decay vertices within inner and outer fiducial volumes were accepted. There were 13 752 events. When weighted to correct for the Λ-length and fiducial cutoffs, the number rose to 15 770 events. The events of the weighted set are plotted in the figures. The loss of events due to scanning inefficiency and measuring difficulties was 6%. This factor is included in cross-section determinations given below. A more detailed presentation of the handling of V + zero-prong events may be found elsewhere.[5]

The spectrum of Fig. 3 shows conspicuous π^0, η, and ω peaks. Figure 4 shows the spectra in the region of the η peak for each of the five K^- momenta. Also shown are the spectra for which the system recoiling against the Λ is produced in the forward direction ($0.8 \leq \cos\theta_{K\eta} \leq 1.0$, where $\theta_{K\eta}$ is the center-of-mass scattering angle) and in the backward direction ($-1.0 \leq \cos\theta_{K\eta} \leq -0.8$). Quite evident in these last panels is the difference in resolution of the η peak. Forward η's correspond to Λ's that are slow in the laboratory system; backward η's correspond to Λ's that are fast. The experimental resolution-function width for events in the η mass region increases by a factor of about four in going from forward η's (slow Λ's) to backward η's (fast Λ's). The resolution-function width also increases, although slowly, with increasing incident K^- momentum. The large variation in the width must be taken into account in determining the number of η's produced at a given angle.

The numbers of events in a band 3Γ wide centered at m_η^2 and in bands 1.5Γ wide to either side[6] were obtained, where Γ is the experimental resolution-function width for events in the η mass region and at the given momentum and angle. Subtracting the number of events in the two side bands from the number in the center band gave the number of η's. Figure 4 shows the results, summed over all angles at each of the momenta and over all momenta in the forward and backward production-angle bins: the number of events above the solid line in each figure is our best estimate for the number of η's, while the dashed lines are drawn one statistical standard deviation to either side. Table II gives numbers of events and cross sections. The production angular distributions are discussed in Sec. IV.

The foregoing procedure for determining the background under the η peak is not entirely satisfactory. Figure 4 shows the limits within which the $\pi^0\gamma$ invariant mass from the reaction $K^-p \rightarrow \Sigma^0\pi^0$, $\Sigma^0 \rightarrow \Lambda\gamma$ can fall. Theoretically, the spectrum for such events is flat within the limits. At all but 1.22 BeV/c, the upper edge of the $\Sigma^0\pi^0$ spectrum lies slightly above the η peak. Therefore the presence of $\Sigma^0\pi^0$ events causes the background of the η peak to be higher than estimated above, and the number of η events smaller. An upper limit to the systematic error can be found by using only the lower of the two background bands to obtain the background to the peak. This upper limit, at each of the momenta, is included in Table II. The systematic error is maximal only when the edge of the $\Sigma^0\pi^0$ spectrum coincides with one of the edges of the band of width 3Γ centered at the η peak. As this is not usually the case, the systematic error should be well within the upper limits.

Our results combined with those of Sec. II are presented in Sec. IV.

IV. COMPARISON AND COMBINATION OF RESULTS

A. Angular Distributions

The angular distributions obtained at 1.51 BeV/c from the two sets of events are compared in Fig. 5. The distributions have been normalized so that the area under each is the same. Although there are about four times as many $\eta \rightarrow$ neutrals events as $\eta \rightarrow \pi^+\pi^-\pi^0$ events, the angular distribution is obtained to about the same accuracy in each case. This of course is because the statistical weight of $\eta \rightarrow$ neutrals events is diminished considerably by the relatively small "signal-to-noise" ratio.

Agreement between the two determinations is even better than might be expected on statistical grounds. Since almost 60% of all the events are at 1.51 BeV/c, this is good indication that, within our statistics, both sets of events lead to accurate determination of the angular distributions. We obtained the final angular distribution at 1.51 BeV/c, shown in Fig. 6, by using least squares to fold together the distributions of Fig. 5. Results at the other momenta, also shown in Fig. 6, were obtained in identical fashion.

The angular distributions were fitted, by using least squares, to the Legendre polynomial series

$$\frac{d\sigma}{d\Omega} = \lambda\!\!\!^{-2} \sum_{n=0}^{n_{max}} a_n P_n(\cos\theta),$$

where $\lambda\!\!\!^{-} = \hbar/q$ is the reduced wavelength in the c.m. system (q is the c.m. momentum). Integration gives the relation $\sigma = 4\pi \lambda\!\!\!^{-2} a_0$. Unfortunately, only at 1.51 BeV/c is the distribution well enough determined to fix the values of n_{max} and the coefficients a_n accurately. There the confidence level that a good fit has been obtained is less than 1% for $n_{max} \leqslant 3$, rises to 13% at $n_{max} \leqslant 4$, to 75% at $n_{max} = 5$, and thereafter decreases. Figure 6 includes the fitted curve for $n_{max} = 5$. The fitted coefficients are

$$a_0 = 0.027 \pm 0.002, \qquad a_1 = 0.011 \pm 0.004,$$
$$a_2 = 0.029 \pm 0.005, \qquad a_3 = 0.026 \pm 0.006,$$
$$a_4 = 0.019 \pm 0.007, \qquad a_5 = 0.020 \pm 0.008.$$

The errors reflect only the uncertainty in shape, not that in normalization. All the coefficients are positive, so all the polynomials add constructively to the peak in the forward direction.

B. Cross Sections

The cross sections obtained from the two sets of events are shown in Fig. 7(a). Agreement is good at 1.51 BeV/c but generally bad elsewhere. Except at 1.70 BeV/c, cross sections obtained from the $\eta \rightarrow$ neutrals events are larger than those obtained from the $\eta \rightarrow \pi^+\pi^-\pi^0$ events. Systematics do indeed cause probable overestimation of the number of $\eta \rightarrow$ neutrals events (see Sec. III). This effect alone, however, is not sufficient to overcome the large differences at 1.22, 1.42, and 1.60 BeV/c; we do not know how to account for them except on the basis of statistics or possible errors in the η branching ratios in Ref. 4. The comparison of cross sections averaged over all momenta is discussed in Sec. V. C in terms of the branching ratio $\Gamma(\eta \rightarrow \text{neutrals})/\Gamma(\eta \rightarrow \pi^+\pi^-\pi^0)$.

Figure 7(b) shows the cross sections obtained by simply folding together the values of Fig. 7(a). Table III summarizes the experimental results. The cross section shows no large variation over the range of this experiment. Results from other experiments, also shown in Fig. 7(b), indicate that the cross section falls off at both higher and lower momenta.

V. CONCLUSIONS

A. $Y_0^*(2100) \rightarrow \Lambda\eta$ Decay

The K^- lab momentum corresponding to total c.m. energy 2100 MeV in the K^-p system is 1.68 BeV/c, so s-channel formation of the $J^P = 7/2^-$ $Y_0^*(2100)$ is possible in this region; see Fig. 8(a). An extreme upper limit for the $Y_0^*(2100)$ coupling to the $\Lambda\eta$ channel can be obtained by assuming that all the cross section near 1.70 BeV/c is due to this diagram. However, two observations permit setting a more stringent limit: (a) There is little evidence for a bump in the cross section near 1.70 BeV/c; (b) the angular distributions are not symmetric about $\theta = 90°$, as they must be if the reaction proceeds entirely through a single partial wave. A somewhat arbitrary but reasonable estimate is that no more than half the cross section is due to $Y_0^*(2100)$ formation and decay. Then the branching fractions $x_{\overline{K}N}$ and $x_{\Lambda\eta}$ of the Y_0^* are related to the cross section (at 1.70 BeV/c) by

$$\frac{\sigma(K^-p \rightarrow \Lambda\eta)}{2} \geqslant \frac{4\pi \lambda\!\!\!^-{}^2 (J+\frac{1}{2})\, x_{\overline{K}N}\, x_{\Lambda\eta}}{2} .$$

The factor 2 in the denominator on the right side occurs because the K^-p system is only one half (in intensity) in the I = 0 channel. Taking $x_{\overline{K}N} = 0.29$,[7] we obtain

$$x_{\Lambda\eta} \leqslant \frac{\sigma(K^-p \rightarrow \Lambda\eta)}{4\pi \lambda\!\!\!^-{}^2 (J+\frac{1}{2})\, x_{\overline{K}N}} ,$$

$$x_{\Lambda\eta} \leqslant \frac{0.29}{8.68 \times 4 \times 0.29} = 0.03.$$

The $Y_0^*(2100)$ decays not more than 3% via the $\Lambda\eta$ channel.

B. Peripheral Production

The most conspicuous feature of the angular distributions is the peak in the forward direction. This indicates the presence and probable dominance of the reaction by t-channel meson-exchange amplitudes; see Fig. 8(b). Conservation laws at the vertices restrict the particles that can be exchanged to I = 1/2 K^*'s having spin-parity J^P in the series $0^+, 1^-, 2^+, \cdots$. The $K^*(890)$ and $K^*(1420)$ satisfy these restrictions. [They are SU(3) companions of the ρ and A_2 mesons, the particles that can be exchanged in the reaction $K^-p \rightarrow \overline{K}^0 n$, which is related by SU(3) to the reaction $K^-p \rightarrow \Lambda\eta$.]

Isotopic-spin 1/2 N^*'s (including the nucleon) can be exchanged in the u channel; see Fig. 8(c). There is no evidence that such exchanges are important here.

C. The Branching Ratio $\Gamma(\eta \to \text{neutrals})/\Gamma(\eta \to \pi^+\pi^-\pi^0)$

The cross section for $K^-p \to \Lambda\eta \to (p\pi^-)(\pi^+\pi^-\pi^0)$, averaged over the momentum distribution of the data, is 37 ± 3 μb. The corresponding cross section with $\eta \to$ neutrals is 148 ± 11 μb, but a systematic overestimation of the $\eta \to$ neutrals of as much as 16% may have been made (see Sec. III). Thus, using all the data, we find that the branching ratio is between 3.2 and 3.8, with a statistical error of 0.4. However, we can substantially reduce the systematic uncertainty in this result by restricting our analysis to events in the forward peak ($\cos\theta_{K\eta} > 0.6$), where the effective resolution-function width in the neutral mass-squared spectra is much narrower than for the entire sample. We find, by the same technique as above, that the branching ratio is between 3.5 and 3.7 with a statistical error of 0.5. Our best estimate of the branching ratio, where we have included both systematic and statistical error, is

$$\frac{\Gamma(\eta \to \text{neutrals})}{\Gamma(\eta \to \pi^+\pi^-\pi^0)} = 3.6 \pm 0.6.$$

This value is consistent with the latest compiled value[4] of 3.25 ± 0.4.

It should be remembered that $\Gamma(\eta \to \text{neutrals})$ is slightly smaller than the sum of the $\pi^0\pi^0\pi^0$, $\gamma\gamma$, and $\pi^0\gamma\gamma$ modes because Dalitz decays (electron-positron pairs at the decay vertex) can occur in all these modes.

These same events have been used to set an upper limit for the branching ratio $\Gamma(\eta \to \pi^+\pi^-\pi^0\gamma)/\Gamma(\eta \to \pi^+\pi^-\pi^0)$ of 7%.[8]

VI. ACKNOWLEDGMENTS

We thank Professor M. Lynn Stevenson and Professor Luis Alvarez for their encouragement and support, and we thank the members of the Scanning and Measuring Group for their contribution to this work.

REFERENCES

*Work done under auspices of the U. S. Atomic Energy Commission.

1. S. M. Flatté, D. O. Huwe, J. J. Murray, J. B. Shafer, F. T. Solmitz, M. Lynn Stevenson, and C. Wohl, Phys. Rev. 145, 1050 (1966).

2. P. Eberhard, S. M. Flatté, D. O. Huwe, J. B. Shafer, F. T. Solmitz, and M. Lynn Stevenson, Phys. Rev. 145, 1062 (1966).

3. G. R. Lynch, Program FAKE: Monte Carlo Simulation of Bubble Chamber Events, Lawrence Radiation Laboratory Report UCRL-10335, 1962 (unpublished).

4. A. H. Rosenfeld, A. Barbaro-Galtieri, W. J. Podolsky, L. R. Price, P. Soding, C. G. Wohl, M. Roos, and W. J. Willis, Rev. Mod. Phys. 39, 1 (1967).

5. C. G. Wohl, K^-p Charge-Exchange Scattering from 1200 to 1700 MeV/c (Ph. D. Thesis), Lawrence Radiation Laboratory Report UCRL-16288, 1965 (unpublished); and C. G. Wohl, M. L. Stevenson, F. T. Solmitz, and L. K. Gershwin, The Reactions $K^-p \rightarrow \overline{K^0}n$ and $K^-p \rightarrow \Lambda\pi^0$ from 1.2 to 1.7 BeV/c and Y^*'s with Spin 7/2, Lawrence Radiation Laboratory Report UCRL-16484, 1967 (unpublished).

6. At backward angles, where Γ is very large, it was necessary to make the side bands only 0.25 Γ wide to keep them from running into the π^0 and ω peak regions.

7. R. L. Cool, G. Giacomelli, T. F. Kycia, B. A. Leontić, K. K. Li, A. Lundby, and J. Teiger, Phys. Rev. Letters 16, 1228 (1966).

8. S. M. Flatté, Search for $\eta \rightarrow \pi^+\pi^-\pi^0\gamma$, Lawrence Radiation Laboratory Report UCRL-17514, April 1967 (submitted to Phys. Rev. Letters).

Table I. Total cross sections for $K^- p \rightarrow \Lambda\eta$ deduced from events for which the Λ decays to $p\pi^-$ and the η decays to $\pi^+\pi^-\pi^0$.

Momentum (BeV/c)	$\sigma_{\Lambda 3\pi}$ [(a)] (μb)	N (3π)	N ($\eta \rightarrow 3\pi$)	$\sigma_{\Lambda\eta}$ [(b)] (μb)
1.22	680 ± 50	428	33.5 ± 8.5	235 ± 60
1.42	2100 ± 60	797	15.5 ± 5.5	185 ± 65
1.51	2260 ± 80	5840	147 ± 15	255 ± 25
1.60	2140 ± 150	644	10 ± 4.5	150 ± 65
1.70	2820 ± 170	1336	38 ± 7	360 ± 70

(a) See Ref. 2.

(b) The branching ratio $\Gamma(\eta \rightarrow \pi^+\pi^-\pi^0)/\Gamma(\eta \rightarrow \text{all}) = 0.224$ has been used.

Table II. Total cross sections for $K^-p \rightarrow \Lambda\eta$ deduced from events for which the Λ decays to $p\pi^-$ and the η decays to neutrals.

Momentum (BeV/c)	Number of events	Cross section[a] (μb)
1.22	149 ± 26 (21)[b]	405 ± 70
1.42	117 ± 23 (11)	360 ± 70
1.51	561 ± 57 (93)	280 ± 30
1.60	111 ± 22 (20)	395 ± 80
1.70	104 ± 28 (17)	235 ± 65

a. Using branching ratios $\Gamma(\Lambda \rightarrow p\pi^-)/\Gamma(\Lambda \rightarrow \text{all}) = 0.664$ and $\Gamma(\eta \rightarrow \text{neutrals})/\Gamma(\eta \rightarrow \text{all}) = 0.729$. See Ref. 4.

b. The number in parentheses is the maximum systematic overestimation of the number of events. See the text.

Table III. Cross sections for the reaction $K^-p \to \Lambda\eta$. The differential cross sections are in μb/sr; their uncertainties are based on the statistics of the angular distributions alone, and do not reflect uncertainties in normalization.

	Momentum (BeV/c)				
cos θ	1.22	1.42	1.51	1.60	1.70
-0.9	40 ± 15	18 ± 18	21 ± 6	34 ± 17	6 ± 13
-0.7	29 ± 16	22 ± 10	25 ± 5	27 ± 10	13 ± 11
-0.5	34 ± 15	10 ± 12	16 ± 4	13 ± 11	11 ± 11
-0.3	4 ± 11	8 ± 12	13 ± 4	-2 ± 11	17 ± 11
-0.1	20 ± 9	10 ± 10	14 ± 4	6 ± 11	4 ± 11
0.1	0 ± 11	6 ± 12	19 ± 4	0 ± 10	40 ± 13
0.3	24 ± 11	4 ± 10	10 ± 4	11 ± 10	19 ± 11
0.5	15 ± 9	12 ± 8	13 ± 4	15 ± 8	25 ± 8
0.7	20 ± 11	24 ± 12	17 ± 4	11 ± 10	21 ± 11
0.9	62 ± 15	87 ± 18	43 ± 7 [a] 79 ± 11	74 ± 17	74 ± 17
σ (μb)	310 ± 45	255 ± 45	265 ± 20	240 ± 50	290 ± 50

a. Bin split; cos θ = 0.85 and 0.95.

FIGURE CAPTIONS

Fig. 1. Three-pion mass spectra around the η region for various incident K^- laboratory momenta. See Table I for our estimates of the number of η's.

Fig. 2. Mass squared of the system recoiling against the $\Lambda\pi^+\pi^-$ system in our $K^-p \rightarrow \Lambda\eta \rightarrow \Lambda\pi^+\pi^-\pi^0$ events. Background has been subtracted. No contamination from $\Lambda\pi^+\pi^-\gamma$ events is seen. The curve is the experimental resolution function for these events, centered on the π^0 mass squared.

Fig. 3. Distribution of $K^-p \rightarrow \Lambda$ + neutrals events, weighted for fiducial-volume and Λ-length cutoffs, versus the square of the invariant mass of the system of undetected neutrals recoiling against the Λ. There are 13 752 events before weighting, and 15 770 after.

Fig. 4. Spectra in the region of the η peak for $K^-p \rightarrow \Lambda$ + neutrals events. Solid lines cutting off the peak delimit our estimates of the number of η events; dashed lines are 1 standard deviation to either side. See the text for how the numbers were obtained.

Fig. 5. Comparison of angular distributions obtained at 1.51 BeV/c from the two sets of events. The distributions have been normalized to the same area.

Fig. 6. Differential cross sections for the reaction $K^-p \rightarrow \Lambda\eta$. The curve at 1.51 BeV/c is taken from a fit to a Legendre polynomial series including terms through $P_5(\cos\theta)$.

Fig. 7. (a) Comparison of $K^-p \rightarrow \Lambda\eta$ cross sections obtained from the two sets of events in our experiment. (b) Cross sections obtained by folding together the results in (a), shown with results of other

experiments. (■) D. Berley, P. L. Connolly, E. L. Hart, D. C. Rahm, D. L. Stonehill, B. Thevenet, W. J. Willis, and S. S. Yamamoto, Phys. Rev. Letters 15, 641 (1965). (□) P. L. Bastien and J. P. Berge, Phys. Rev. Letters 10, 188 (1963). (▲) W. P. Trower (Ph. D. Thesis), Urbana, Illinois, 1966. (▼) P. M. Dauber, W. M. Dunwoodie, P. E. Schlein, W. E. Slater, L. T. Smith, D. H. Stork, and H. K. Ticho, in Proceedings of the Second Topical Conference on Resonant Particles, p. 380, Athens, Ohio, 1965. (△) G. W. London, R. R. Rau, N. P. Samios, S. S. Yamamoto, M. Goldberg, S. Lichtman, M. Prime, and J. Leitner, Phys. Rev. 143, B1034 (1966). (▽) S. M. Flatté, Phys. Rev. 155, 1517 (1967). [The η fractions in the $\Lambda\pi^+\pi^-\pi^0$ final state were determined from the mass plots in this reference. A branching fraction of 0.224 for $\eta \to \pi^+\pi^-\pi^0$ was then used to get $\sigma(\Lambda\eta)$.]

Fig. 8. Feynman diagrams representing exchanges in the three channels that affect $K^-p \to \Lambda\eta$: (a) s-channel exchange; (b) t-channel exchange; (c) u-channel exchange.

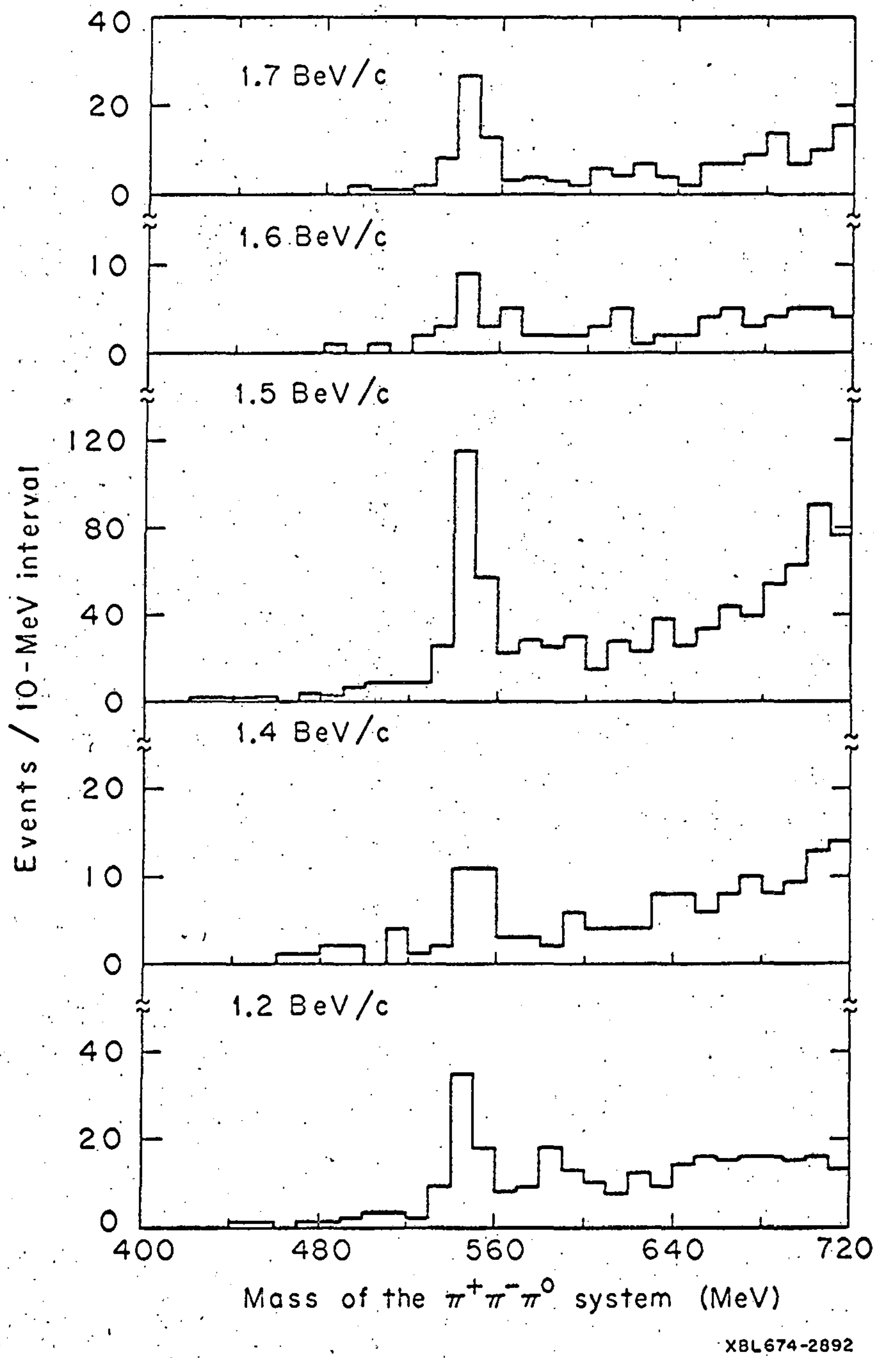

1.7 BeV/c
1.6 BeV/c
1.5 BeV/c
1.4 BeV/c
1.2 BeV/c
Events / 10-MeV interval
Mass of the $\pi^+\pi^-\pi^0$ system (MeV)
400
480
560
640
720
XBL674-2892

Fig. 1

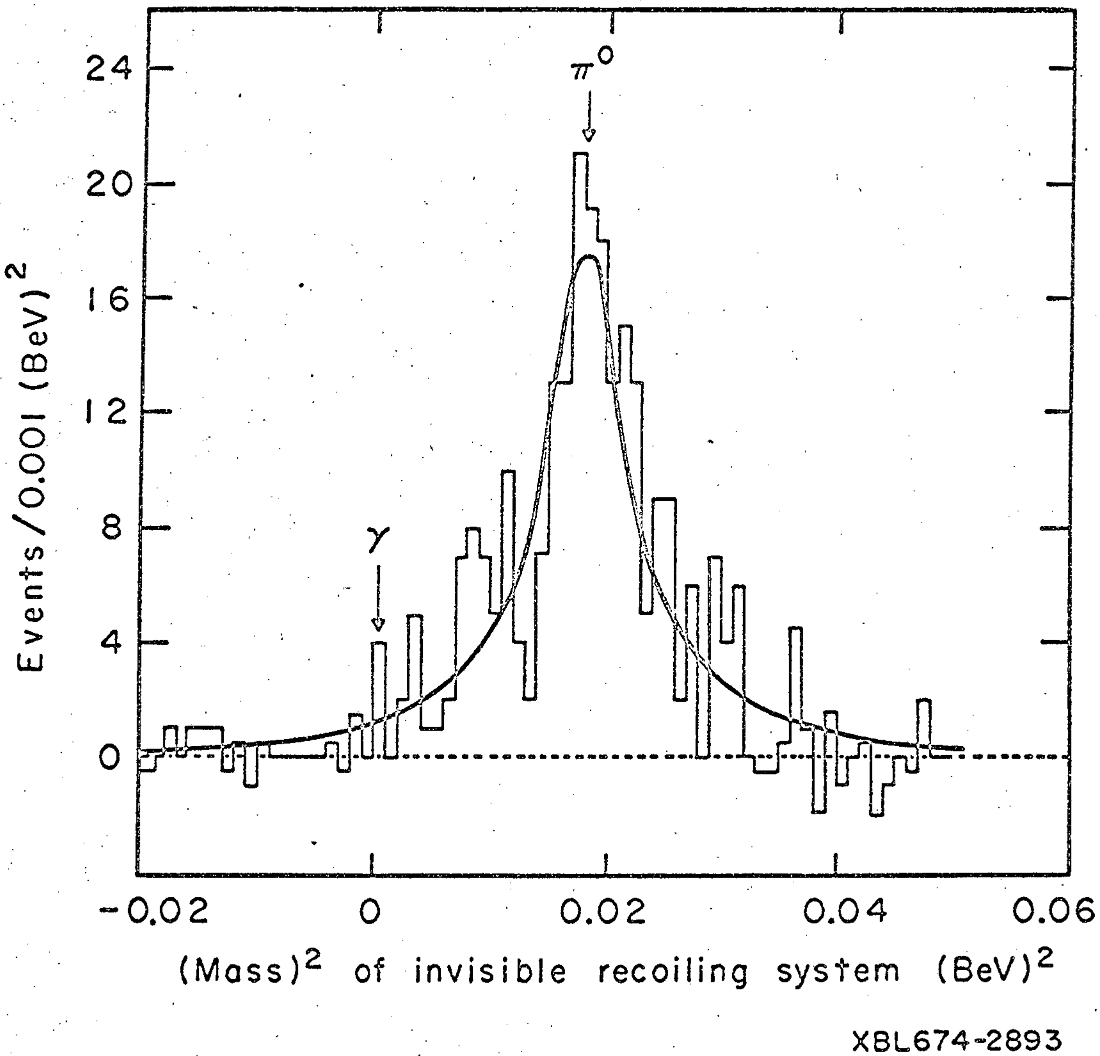
24
20
16
12
8
4
0
Events/0.001 (BeV)^2
π^0
γ
-0.02
0
0.02
0.04
0.06
(Mass)^2 of invisible recoiling system (BeV)^2
XBL674-2893

Fig. 2

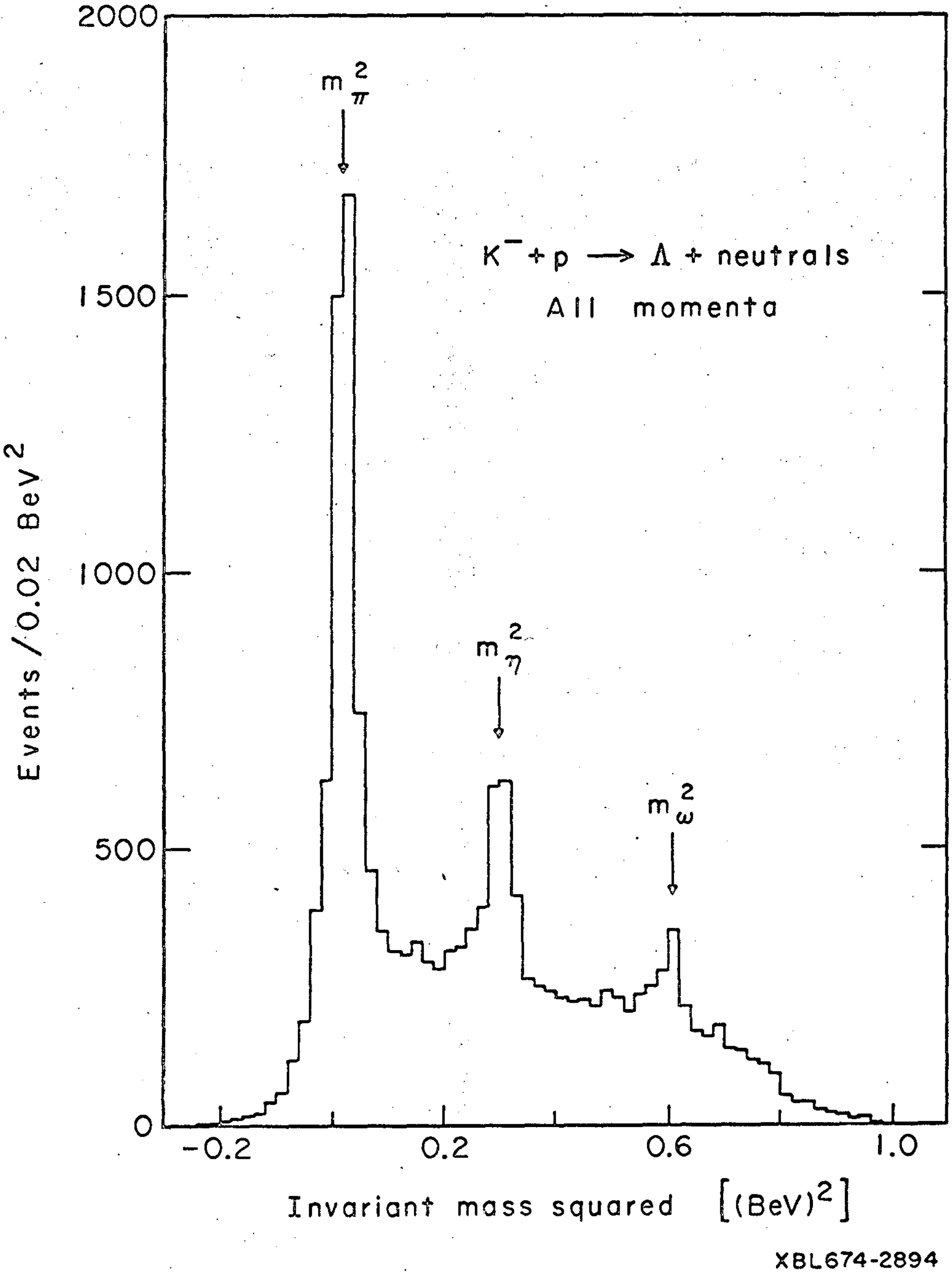
2000
1500
1000
500
0
Events /0.02 BeV^2
m_π^2
m_η^2
m_ω^2
$K^- + p \longrightarrow \Lambda$ + neutrals
All momenta
-0.2
0.2
0.6
1.0
Invariant mass squared [(BeV)^2]
XBL674-2894

Fig. 3

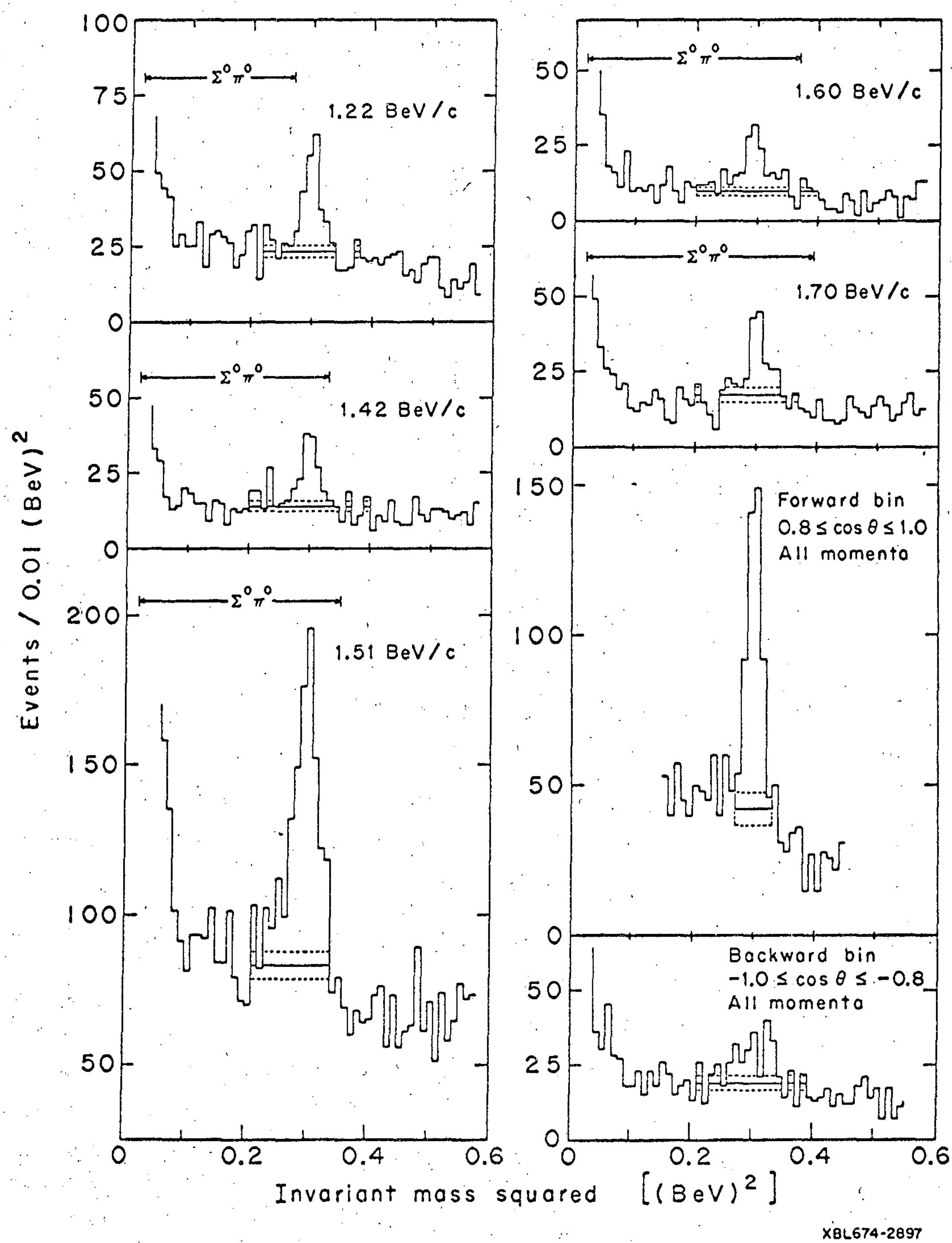

Σ°π°
1.22 BeV/c
1.42 BeV/c
1.51 BeV/c
1.60 BeV/c
1.70 BeV/c
Forward bin
0.8 ≤ cos θ ≤ 1.0
All momenta
Backward bin
-1.0 ≤ cos θ ≤ -0.8
All momenta
Events / 0.01 (BeV)^2
Invariant mass squared [(BeV)^2]
XBL674-2897

Fig. 4

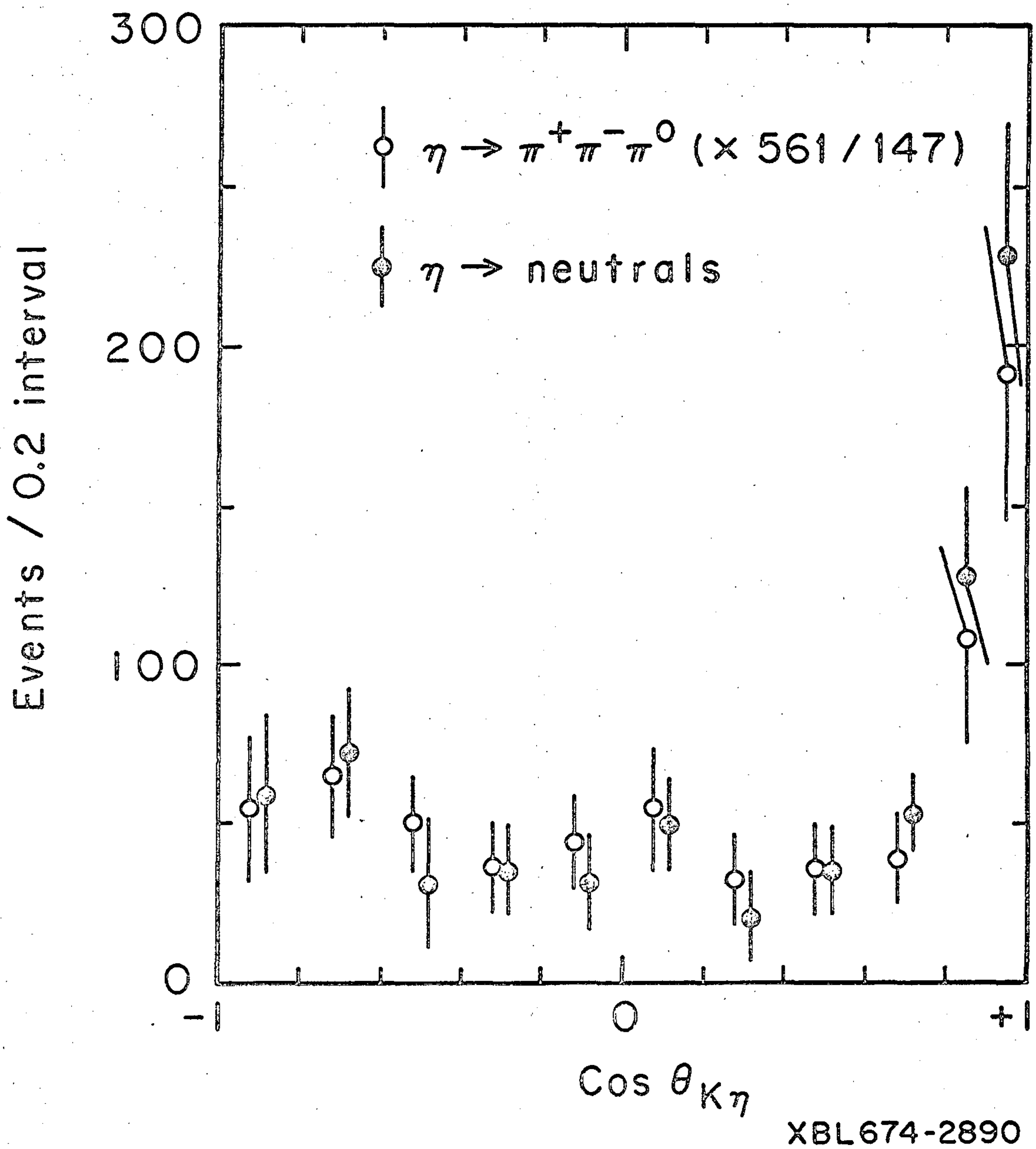
300
200
100
0
Events / 0.2 interval
$\eta \rightarrow \pi^+\pi^-\pi^0$ (× 561/147)
$\eta \rightarrow$ neutrals
-1
0
+1
Cos $\theta_{K\eta}$
XBL674-2890

Fig. 5

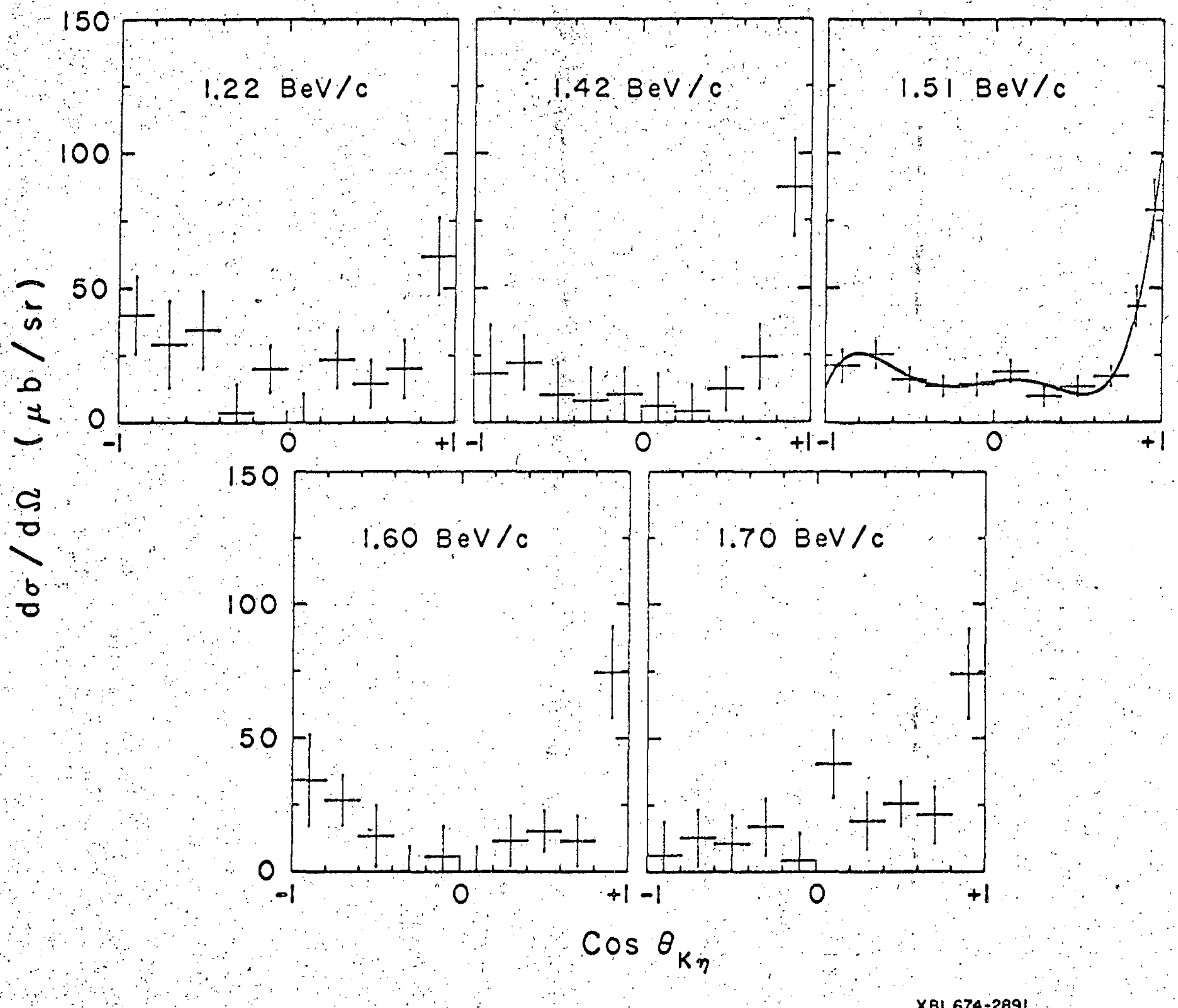
150
100
50
0
1.22 BeV/c
1.42 BeV/c
1.51 BeV/c
1.60 BeV/c
1.70 BeV/c
-1
0
+1
dσ/dΩ (μb/sr)
Cos $\theta_{K\eta}$
XBL 674-2891

Fig. 6

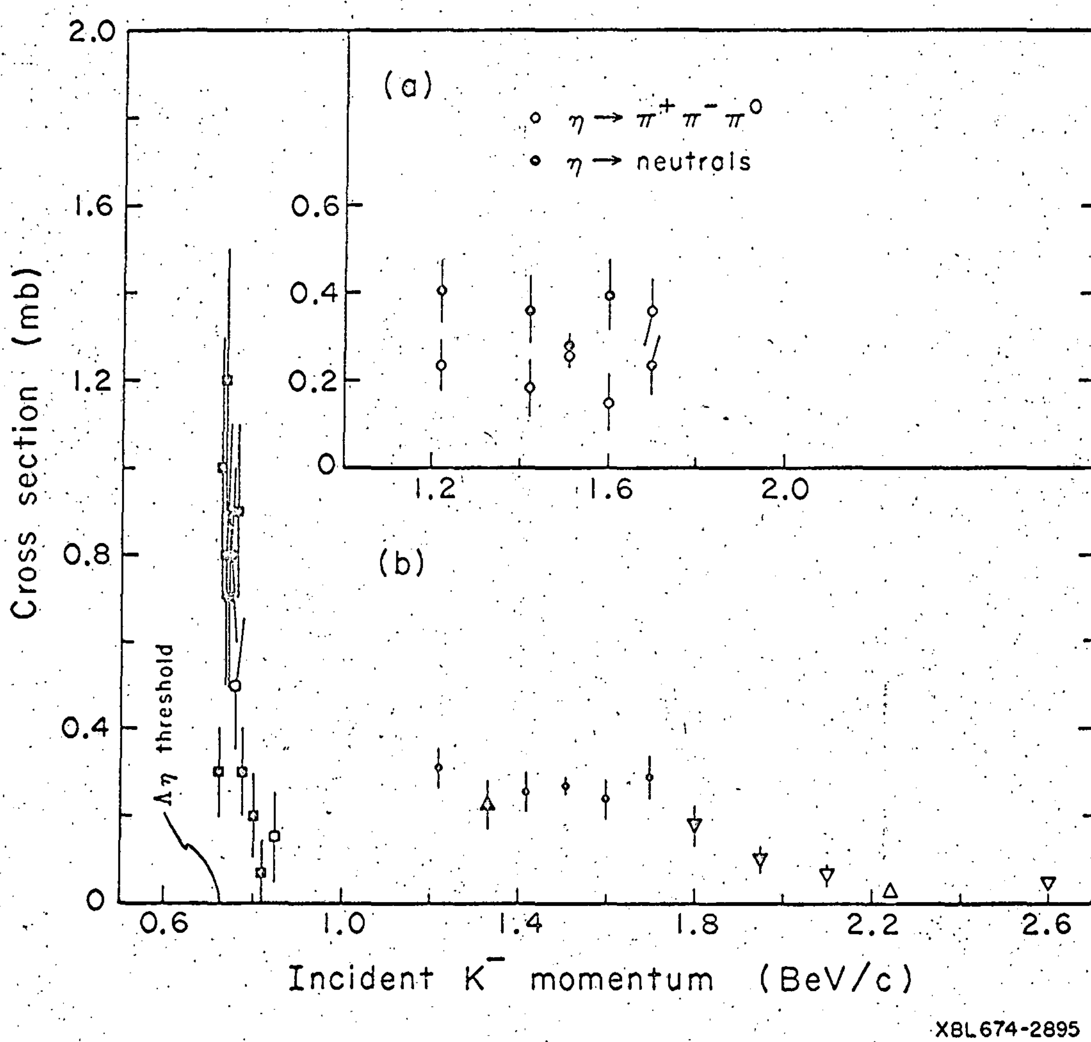
(a)
η → π⁺π⁻π⁰
η → neutrals
0.6
0.4
0.2
0
1.2
1.6
2.0
(b)
2.0
1.6
1.2
0.8
0.4
0
0.6
1.0
1.4
1.8
2.2
2.6
Cross section (mb)
Λη threshold
Incident K⁻ momentum (BeV/c)
XBL674-2895

Fig. 7

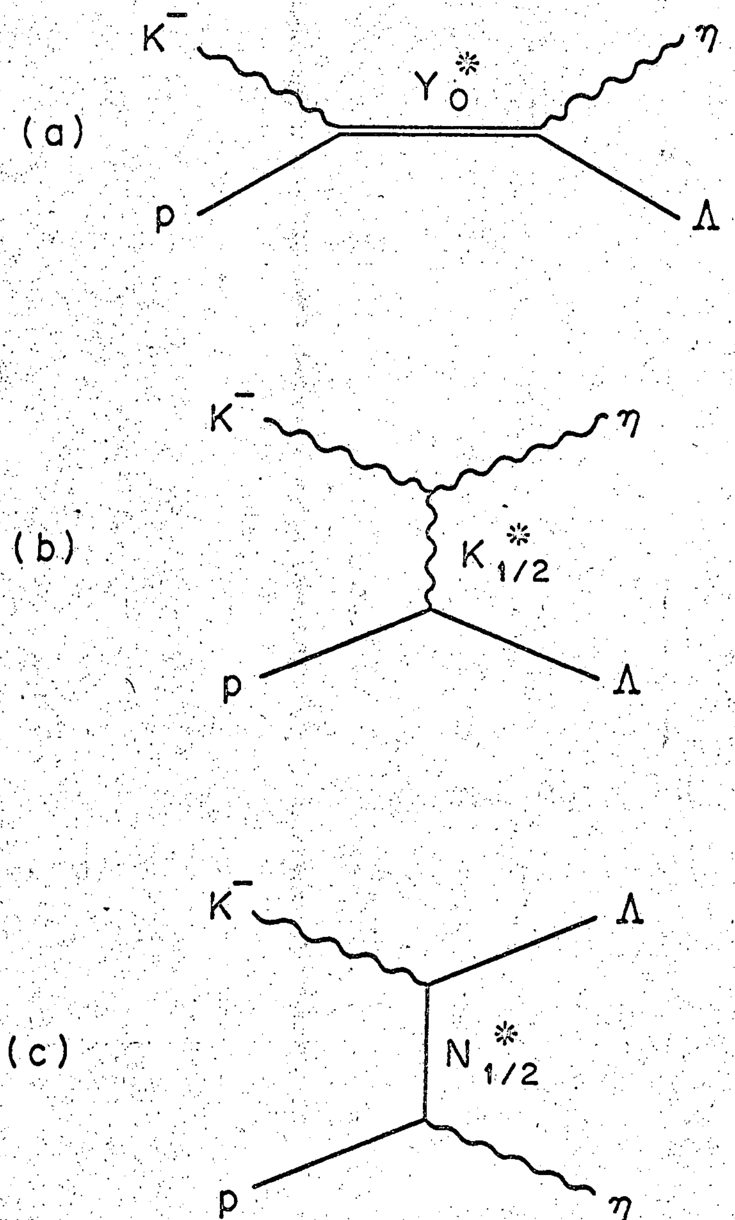

XBL674-2896

Fig. 8